Cooperative circumnavigation for a mobile target using adaptive estimation

Joana Fonseca[1], Jieqiang Wei[2], Tor A. Johansen[3], and Karl H. Johansson[1]

[1] KTH Royal Institute of Technology, Stockholm, Sweden, {jfgf,kallej}@kth.se,
[2] Ericsson, Stockholm, Sweden, jieqiang.wei@ericsson.com,
[3] Norwegian University of Science and Technology, Trondheim, Norway, tor.arne.johansen@ntnu.no,

Abstract. In this paper we consider the problem of tracking a mobile target using adaptive estimation while circumnavigating it with a system of Unmanned Surface Vehicles (USVs). The mobile target considered is an irregular dynamic shape approximated by a circle with moving centre and varying radius. The USV system is composed of n USVs of which one is equipped with an Unmanned Aerial Vehicle (UAV) capable of measuring both the distance to the boundary of the target and to its centre. This USV equipped with the UAV uses adaptive estimation to calculate the location and size of the mobile target. The USV system must circumnavigate the boundary of the target while forming a regular polygon. We design two algorithms: One for the adaptive estimation of the target using the UAV's measurements and another for the control protocol to be applied by all USVs in their navigation. The convergence of both algorithms to the desired state is proved up to a limit bound. Two simulated examples are provided to verify the performance of the algorithms designed in this paper.

1 Introduction

The use of unmanned vehicles has allowed higher levels of precision and cost efficiency in many research expeditions [1]. It is particularly relevant in challenging or hazardous environments, and if real-time data exchange is required [2]. The solution of the future relies on the connection of different types of unmanned vehicles. In [3] it is stated that autonomous systems are becoming more powerful and utilise the capabilities of several types of devices such as Unmanned Aerial Vehicles (UAVs) and Unmanned Surface Vehicles (USVs). The opportunity for coordinated and interconnected operations is clear. Hence, we believe a good solution relies on a coordinated and interconnected system of USVs and one UAV and using an adaptive protocol. In [4] a path following algorithm is proposed for formation control of a multi-agent system. The authors prove that if the tracking errors are bounded, their method stabilises the formation error. However, it is assumed that there is perfect information on the path to follow. For our problem, we would like to estimate the target, design the path and control the multi-USV system. In [5], [6] and [7] a control law for distance-based formation control which guarantees stability is proposed. Also in section 6.3.1 of [8], where target tracking is considered, they use distance-based formation control. However, a distance-based protocol can not fit into our target tracking problem since it does not use global information. In [9] a protocol for target

tracking in 3D is designed with guaranteed collision avoidance. However, it is assumed that the target is a fixed object that may move and rotate but never change its shape, which is different from our case. In [10] and [11], controllers are synthesised for a swarm of agents to generate a desired two-dimensional geometric pattern specified by a simple closed planar curve. It is assumed that the shape is given to the swarm and not estimated in real-time. This is not true for our case. A closely related work [12] proposed one adaptive protocol to circumnavigate around a moving point, e.g., the fish tracking problem. They used adaptive estimation for point tracking with known constant distance. We shall extend this to circumnavigation of circular shapes.

The main contribution of this paper is the original setup, the estimation protocol, the control algorithm and the convergence and numerical results. The setup of this paper consists on a multi-USV system paired up with an UAV. This setup intends to construct a powerful system by using the unique capabilities of each type of autonomous vehicle such that we can both analyse the target and USV's location (using the UAV) but also analyse the different fronts of the target (using the USVs). The estimation protocol we developed estimates the target centre and radius for each time instance in real time. We use adaptive filtering that relies on the distance measurements collected by the UAV, assuming its movement is persistently exciting for all time. The control algorithm we propose for each USV gives us mathematical guarantees of bounded convergence to the target and to equally spaced positions along it, accounting for physical restrictions for implementation. We simulated this proposed system using a man made random data set to represent a circular target. The current paper significantly extends our IROS 2019 publication [13], which focuses on how to circumnavigate an algal bloom shape. In both we wish to track a circular shape but the assumptions, methods and results are different. In our previous paper, we assumed that all USVs are able to measure only the distance to the boundary. The algorithm was based on least squares optimisation for estimating the circle and we apply the controller to an algal bloom data set. Whereas on the present paper we assume only one sensing USV that measures distance to the boundary as well as centre and our algorithm uses adaptive estimation.

The remaining sections of this paper are organised as follows. In Section 2, the main problem of interest is formulated. It is divided in system description and problem formulation. The main results are presented in Section 3, where the adaptive estimation and control algorithm are derived. In Section 4 we present the proofs of convergence. Simulations presenting the performance of the proposed algorithm are given in Section 5. It is divided in simulations with and without p.e. guarantees. Concluding remarks and future directions come in Section 6.

2 System description and problem formulation

In this paper we consider the problem of tracking a shape using a multi-USV system and an UAV. This shape may be very irregular over time. We assume the shape is close to a circle as seen in Fig. 1. The UAV provides an initial image of the target which confirms such assumption and helps us deploy the USVs.

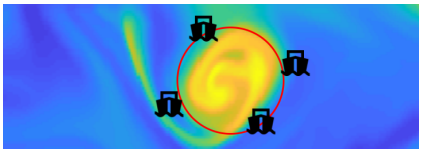

Fig. 1: 4 USVs circumnavigating a circular algal bloom

2.1 System description

We define this circle as $(\mathbf{c}(t), r(t)) \in \mathbb{R}^3$, where $\mathbf{c}(t) = (x(t), y(t))$ and $r(t)$ are the centre and the radius of the circle, respectively. We denote $(\hat{\mathbf{c}}(t), \hat{r}(t)) \in \mathbb{R}^3$ as the estimation of the circle attributes. Then the UAV would provide initial estimates $\hat{\mathbf{c}}(0) = (\hat{x}(0), \hat{y}(0))$ and $\hat{r}(0)$.

This UAV obtains data from the target and shares it with the USVs so they can move towards the target. The UAV constantly measures its distance from the target, calculates its target estimates and shares it with all USVs. The measurements consist of its distance to the centre and to its boundary. Each USV has access to its GPS position and to the GPS position of the USV in front of it, counterclockwise with respect to $\hat{\mathbf{c}}(t)$.

The multi-USV system will jointly circumnavigate the target and provide real time information of different fronts. We define we have n USVs and, using the UAV information, they are initialised at positions $\mathbf{p}_i(0)$, $i \in [1, ..., n]$, which are outside of the shape and form a counterclockwise directed ring on the surface. The kinematic of the USVs is of the form

$$\dot{\mathbf{p}}_i = \mathbf{u}_i, \qquad i \in [1, ..., n], \tag{1}$$

where $\mathbf{p}_i$ is a vector that contains the position $\mathbf{p}_i = [x_i, y_i]^\top \in \mathbb{R}^2$ and $\mathbf{u}_i \in \mathbb{R}^2$ is the control input.

In order to avoid the USVs concentrating in some region, in which case they may loose information on other fronts, we would like to space them equally along the defined circle. Therefore, we define that the counterclockwise angle between the vector $\mathbf{p}_i - \hat{\mathbf{c}}$ and $\mathbf{p}_{i+1} - \hat{\mathbf{c}}$ is denoted as $\beta_i = \angle(\mathbf{p}_{i+1} - \hat{\mathbf{c}}, \mathbf{p}_i - \hat{\mathbf{c}})$ for $i = 1, \ldots, n-1$, and the angle between $\mathbf{p}_n - \hat{\mathbf{c}}$ and $\mathbf{p}_1 - \hat{\mathbf{c}}$ is denoted as $\beta_n = \angle(\mathbf{p}_1 - \hat{\mathbf{c}}, \mathbf{p}_n - \hat{\mathbf{c}}) = \angle(\mathbf{p}_1 - \hat{\mathbf{c}}, \mathbf{p}_n - \hat{\mathbf{c}})$, Notice that in this case, $\beta_i(0) \geq 0$ and $\sum_{i=1}^{n} \beta_i(0) = 2\pi$. This is represented in the left scheme of Fig. 2.

Note that the ℓ_2-norm is denoted simply as $\|\cdot\|$ without a subscript. Now we can define the distance from the UAV to the centre and the boundary of the target circle as

$$\begin{aligned} D_1^c(t) &= \|\mathbf{c}(t) - \mathbf{p}_1(t)\| \\ D_1^b(t) &= |r(t) - D_1^c(t)|, \end{aligned} \tag{2}$$

respectively. Note that this UAV is capable of sensing the distances to the target but then calculates the target estimates. This UAV operation is represented in the left part of Fig. 3.

After obtaining the target estimates, each USV i would be able to calculate its own distances $\hat{D}_i^c(t) = \|\hat{\mathbf{c}}(t) - \mathbf{p}_i(t)\|$ and $\hat{D}_i^b(t) = |\hat{r}(t) - \hat{D}_i^c(t)|$ as represented in the right scheme of Fig. 2. We summarise each USVs' scheme of computation in the right part of Fig. 3.

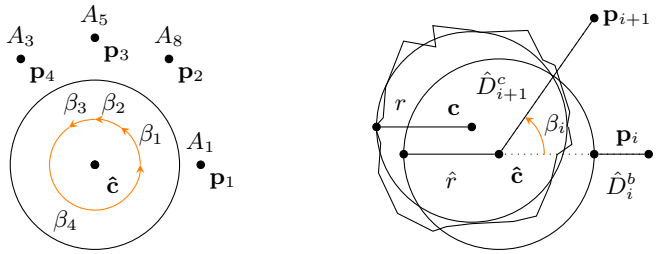

Fig. 2: (Left) System with vehicles A_1, A_3, A_5, A_8 at positions $\mathbf{p}_1$, $\mathbf{p}_4$, $\mathbf{p}_3$, $\mathbf{p}_2$, respectively. (Right) Estimated $\hat{\mathbf{c}}$, $\hat{r}$, real $\mathbf{c}$, r and angle β_i between two vehicles at $\mathbf{p}_{i+1}$ and $\mathbf{p}_i$.

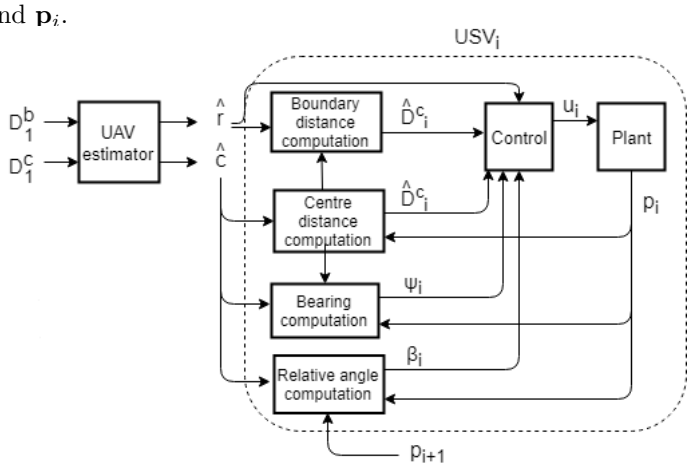

Fig. 3: The UAV estimates the centre and radius of the target using its distance measurements and shares it with all USVs. Each USV i calculates its control protocol.

2.2 Problem formulation

Definition 1 (Circumnavigation). *When the target is stationary, i.e.,* $\mathbf{c}$ *and* r *are constant, circumnavigation is achieved if the USVs*

1. *move in a counterclockwise direction on the boundary of the target, and*
2. *are equally distributed along the circle, i.e.,* $\beta_i = \frac{2\pi}{n}$.

More precisely, we say that the circumnavigation is achieved asymptotically if the previous aim is satisfied for $t \to \infty$. *For the case with time-varying target, we assume that* $\|\dot{\mathbf{c}}\| \leq \varepsilon_1$ *and* $|\dot{r}| \leq \varepsilon_2$ *for some positive constant* ε_1 *and* ε_2.

Now we are ready to pose the problem of interest.

Problem 1. Design a UAV estimator for $\mathbf{c}(t)$ and $r(t)$ when distance measures (2) are available to the UAV, and design the control input $\mathbf{u}_i$ for the USVs such that for some positive ε_1, ε_2 we have $\|\dot{\mathbf{c}}\| \leq \varepsilon_1$ and $|\dot{r}| \leq \varepsilon_2$. Then, there exist positive K_1, K_2 and K_3 satisfying

$$\limsup_{t\to\infty} \|\hat{\mathbf{c}}(t) - \mathbf{c}(t)\| \leq K_1\varepsilon_1, \quad \limsup_{t\to\infty} |\hat{r}(t) - r(t)| \leq K_2\varepsilon_2,$$
$$\limsup_{t\to\infty} |\hat{D}^c_i(t) - \hat{r}(t)| \leq K_3\varepsilon_2,$$
$$\lim_{t\to\infty} \beta_i(t) = \frac{2\pi}{n}.$$

3 Adaptive estimation and control algorithms

In this section, we propose an estimation and control mechanism for Problem 1. We consider n USVs at positions $\mathbf{p}_i$ and one UAV which is capable of measuring its distance D_i^b to the target boundary as well as its distance D_i^c to the target centre. Then, it should estimate $(\mathbf{c}, r)$ from its distance measures, i.e. D_i^b and D_i^c, and share the information with the USVs. Each USV calculates its desired velocity taking into account its angle β_i to the next USV as well as its distance to the target centre and boundary, obtained with the estimates of the target.

3.1 Adaptive estimation

This subsection relates to the protocol followed by the UAV for estimation. Recalling Fig. 3, we will construct the UAV estimator block. Motivated by [12], we propose the following adaptive estimation of the radius $r(t)$ of the target using the UAV A_1 in position $\mathbf{p}_1$. Observe that

$$\frac{d}{dt}(D_1^b)^2 = 2(\dot{r} - \dot{D}_1^c)(r - D_1^c). \tag{3}$$

Assume the estimate of r is denoted as $\hat{r}$, we have

$$\frac{1}{2}\big(\frac{d}{dt}(D_1^b)^2 - \frac{d}{dt}(D_1^c)^2\big) + \dot{D}_1^c\hat{r} = \dot{D}_1^c(\hat{r} - r) + \dot{r}(r - D_1^c). \tag{4}$$

Then for some positive constant γ the dynamic

$$\dot{\hat{r}} = -\gamma\dot{D}_1^c\big[\frac{1}{2}\big(\frac{d}{dt}(D_1^b)^2 - \frac{d}{dt}(D_1^c)^2\big) + \dot{D}_1^c\hat{r}\big] \tag{5}$$

can estimate the variable r under the persistent excitation condition on $\dot{D}_1^c$. Persistent excitation plays a key role in establishing parameter convergence in adaptive identification [14,15].

Definition 2. *(Continuous time persistent excitation condition) [15] The function* $f \in_e^2 (\mathbb{R}^n)$ *is said to be* persistently exciting (p.e.) *if there exist positive constants* ε_1, T *such that for all* $\tau > 0$,

$$\int_\tau^{T+\tau} f(t)f(t)^\top dt > \varepsilon_1 I_n.$$

T *will be termed an excitation period of* f.

Indeed, in this case $\frac{d}{dt}(\hat{r} - r) = -\gamma(\dot{D}_1^c)^2(\hat{r} - r) - \vartheta_{\dot{r}}$, where $\vartheta_{\dot{r}} = \dot{r}(\gamma\dot{D}_1^c(r - D_1^c) + 1)$ is bounded by $M_1\varepsilon_2$. Indeed all its elements are bounded by M_1 and recall that $|\dot{r}| \leq \varepsilon_2$. Note that $r - D_1^c$ is bounded because r and D_1^c are bounded as well. Furthermore, as it will be clear soon, $\vartheta_{\dot{r}}$ can be replaced by $\vartheta_{\dot{r}} = \dot{r}(\gamma V(r - D_1^c) + 1)$ using equation (8), where V is the bounded estimate of $\dot{D}_1^c$.

However, the implementation of (5) needs the derivative of D_1^b and D_1^c which is not desired. It would require explicit differentiation of measured signals with accompanying noise amplification. Thus, for some positive constant α we adopt the state variable filtering and then design the estimator as follows

$$\eta(t) = \dot{z}_1 = -\alpha z_1(t) + \frac{1}{2}(D_1^b)^2 \tag{6}$$

$$m(t) = \dot{z}_2 = -\alpha z_2(t) + \frac{1}{2}(D_1^c)^2 \tag{7}$$

$$V(t) = \dot{z}_3 = -\alpha z_3(t) + D_1^c \tag{8}$$

with initial conditions $z_1(0) = z_2(0) = z_3(0) = 0$. Now together the above dynamics, the estimator for r is given as

$$\dot{\hat{r}} = -\gamma V\big[\eta - m + V\hat{r}\big]. \tag{9}$$

Now we need to know $\mathbf{c}(t)$ but we only know $D_1^c(t)$ and $D_1^b(t)$. Thus, we must use again adaptive estimation for the centre $\mathbf{c}(t)$ of the target. Observe that

$$\frac{d}{dt}(D_1^c)^2 = 2(\dot{\mathbf{p}}_1 - \dot{\mathbf{c}})^\top(\mathbf{p}_1 - \mathbf{c}). \tag{10}$$

Assume the estimation of $\mathbf{c}$ is denoted as $\hat{\mathbf{c}}$, we have

$$\frac{1}{2}\big(\frac{d}{dt}(D_1^c)^2 - \frac{d}{dt}\|\mathbf{p}_1\|^2\big) + \dot{\mathbf{p}}_1^\top\hat{\mathbf{c}} = \dot{\mathbf{p}}_1^\top(\hat{\mathbf{c}} - \mathbf{c}) + \dot{\mathbf{c}}^\top(\mathbf{c} - \mathbf{p}_1). \tag{11}$$

Then the dynamic

$$\dot{\hat{\mathbf{c}}} = -\gamma\dot{\mathbf{p}}_1\big[\frac{1}{2}\big(\frac{d}{dt}(D_1^c)^2 - \frac{d}{dt}\|\mathbf{p}_1\|^2\big) + \dot{\mathbf{p}}_1^\top\hat{\mathbf{c}}\big] \tag{12}$$

can estimate the parameter $\mathbf{c}$ under some persistent excitation condition on $\dot{\mathbf{p}}_1$. Indeed, in this case

$$\frac{d}{dt}(\hat{\mathbf{c}} - \mathbf{c}) = -\gamma\|\dot{\mathbf{p}}_1\|^2(\hat{\mathbf{c}} - \mathbf{c}) - \vartheta_{\dot{\mathbf{c}}}, \tag{13}$$

where $\vartheta_{\dot{\mathbf{c}}} = \gamma\dot{\mathbf{c}}^\top\dot{\mathbf{p}}_1(\mathbf{c} - \mathbf{p}_1) + \dot{\mathbf{c}}$ is bounded by $M_2\varepsilon_1$. Indeed all its elements are bounded by M_2 and recall that $|\dot{\mathbf{c}}| \leq \varepsilon_1$. Note that $\mathbf{c} - \mathbf{p}_1$ is bounded because $\mathbf{c}$ and $\mathbf{p}_1$ are within a finite map. Furthermore, as it will be clear soon, $\vartheta_{\dot{\mathbf{c}}}$ can be replaced by $\vartheta_{\dot{\mathbf{c}}} = \gamma\dot{\mathbf{c}}^\top V_2(\mathbf{c} - \mathbf{p}_1) + \dot{\mathbf{c}}$ using equation (15), where V_2 is the estimate of $\dot{\mathbf{p}}_1$ and it is bounded.

However, the implementation of (12) needs the derivative of $\mathbf{p}_1(t)$ and $D_1^c(t)$ which is not desired. Therefore we use the previously defined equation (7) for $D_1^c(t)$ and redefine it as $\eta_2(t) = \dot{z}_2$ and add the following filter

$$m_2(t) = \dot{z}_4 = -\alpha z_4(t) + \frac{1}{2}\mathbf{p}_1(t)\mathbf{p}_1^T(t) \tag{14}$$

$$V_2(t) = \dot{z}_5 = -\alpha z_5(t) + \mathbf{p}_1(t) \tag{15}$$

with initial conditions $z_4(0) = z_5(0) = 0$. Now together the above dynamics, the estimator for $\mathbf{c}$ is given as

$$\dot{\hat{\mathbf{c}}} = -\gamma V_2\big[\eta_2 - m_2 + V_2^T\hat{\mathbf{c}}\big]. \tag{16}$$

3.2 Control algorithm

This subsection relates to the protocol followed by the USVs for control. Recalling Fig. 3, we will construct the USV control block. Therefore, we want to obtain the desired control input $\mathbf{u}_i(t)$ using the previously measured and estimated variables. The total velocity of each USV comprises of two sub-tasks: approaching the target and circumnavigating it. Therefore we define the direction of each USV towards the estimated centre of the target as the bearing $\boldsymbol{\psi}_i(t)$,

$$\boldsymbol{\psi}_i(t) = \frac{\hat{\mathbf{c}}(t) - \mathbf{p}_i(t)}{\hat{D_i^c}(t)} = \frac{\hat{\mathbf{c}}(t) - \mathbf{p}_i(t)}{\|\hat{\mathbf{c}}(t) - \mathbf{p}_i(t)\|}. \tag{17}$$

The first sub-task is related to the bearing $\boldsymbol{\psi}_i(t)$ and the second one is related to its perpendicular, $E\boldsymbol{\psi}_i(t)$. We define a rotation matrix $E = \begin{bmatrix} 0 & 1 \\ -1 & 0 \end{bmatrix}$.

Then, let us first consider the control law $\mathbf{u}_i$ where δ is a parameter to be defined.

$$\mathbf{u}_i = \dot{\hat{\mathbf{c}}} + ((\hat{D}_i^c - \hat{r}) - \frac{1}{\delta}\dot{\hat{r}})\boldsymbol{\psi}_i + \beta_i \hat{D}_i^c E\boldsymbol{\psi}_i \tag{18}$$

The control actuation of a USV is limited, therefore we have to make sure that the implemented control is within the actuation bounds and so we introduce

$$\mathbf{u}_i = \delta \mathbf{u}_i \tag{19}$$

where δ is the same as before. For a specific $\mathbf{u}_i$ it is possible to have $\mathbf{u}_i$ within some specified bounds.

4 Convergence results

In this section we prove that the estimator and control algorithm proposed in the previous section converge to the desired behaviour.

Theorem 1. *The initial condition satisfies $\hat{D}_i^c(0) > \hat{r}(0) > 0$. Suppose $\dot{\mathbf{p}}_1(t)$ and $\dot{D}_1^c(t)$ are p.e., $\|\dot{\mathbf{c}}\| \leq \varepsilon_1$, and $|\dot{r}| \leq \varepsilon_2$. Consider the system (1) with the control protocol (19), and the initialisation satisfying $\|\mathbf{p}_i(0) - \hat{\mathbf{c}}(0)\| > 0$, then there exists K_1, K_2 and K_3 such that circumnavigation of the moving circle with equally spaced USVs can be achieved asymptotically up to a bounded error, i.e.*

$$\limsup_{t\to\infty} \|\hat{\mathbf{c}}(t) - \mathbf{c}(t)\| \leq K_1\varepsilon_1, \tag{20}$$

$$\limsup_{t\to\infty} |\hat{r}(t) - r(t)| \leq K_2\varepsilon_2, \tag{21}$$

$$\limsup_{t\to\infty} |\hat{D}_i^c(t) - \hat{r}(t)| \leq K_3\varepsilon_2, \tag{22}$$

$$\lim_{t\to\infty} \beta_i(t) = \frac{2\pi}{n}. \tag{23}$$

Proof. The proof is divided into three parts. In the first part, we prove that (20) and (21) hold. In the second part, we prove that the estimated distance $\hat{D}_i^c$ converges to the estimated radius $\hat{r}$, or in other words, that (22) holds. In the last part, we show that the angle between the USVs will converge to the average consensus for n USVs, $\beta_i = \frac{2\pi}{n}$, meaning (23) holds. We will assume the implementable controller is given by $\mathbf{U}_i = \delta\mathbf{u}_i$.

1. Firstly, we prove that (20) and (21) hold. The proof for boundedness of the centre (20), can be found on [12], Proposition 7.1. The proof for boundedness of the radius, however, needs to be derived in this paper. Then, we have that

$$\begin{aligned}\dot{\tilde{r}} = \dot{\hat{r}} &= -\gamma V\big[\eta - m + V\hat{r}\big] = -\gamma V\big[\eta - m + V(\tilde{r} + r)\big] \\ &= -\gamma V^2\tilde{r} - \gamma V\big[\eta - m + Vr\big] = -\gamma V^2\tilde{r} + G(t)\end{aligned}$$

   where $G(t) = -\gamma V\big[\eta - m + Vr\big]$. We know that $|G(t)| \leq k_1\epsilon_2$ for some $k_1, \epsilon_2 \geq 0$ because V is bounded and that $|\eta - m + Vr| < k_2$ we can prove that for a Lyapunov function $W_r = \frac{1}{2}\tilde{r}^2$ we get

$$\begin{aligned}\dot{W}_r = \tilde{r}\dot{\tilde{r}} &= \tilde{r}(-\gamma V^2\tilde{r} + G(t)) = -\gamma V^2\tilde{r}^2 + \tilde{r}G(t) \\ &\leq -\gamma V^2\tilde{r}^2 + k_1\epsilon_2\tilde{r}\end{aligned}$$

   then we get that for $\dot{W}_r \leq 0$ to hold, $-\gamma V^2\tilde{r}^2 + k_1\epsilon_2\tilde{r} \leq 0$ must hold. So, we have that when $\tilde{r} \geq \frac{k_1\epsilon_2}{\gamma V^2}$ or $\tilde{r} \leq -\frac{k_1\epsilon_2}{\gamma V^2}$, $\dot{W}_r \leq 0$ so that $|\tilde{r}|$ is within $\pm\frac{k_1\epsilon_2}{\gamma V^2}$. This error $\tilde{r}$ is then proved to converge asymptotically to a ball since $\dot{D}_1^c$ is p.e.

2. We prove that all USVs reach the estimate of the boundary of the moving circles asymptotically, i.e., $\lim_{t\to\infty}\|\mathbf{p}_i(t)-\hat{\mathbf{c}}(t)\| = \lim_{t\to\infty}\hat{D}_i^c(t) = \hat{r}(t)$, so (22) holds. Consider the function $W_i(t) := \hat{D}_i^c(t) - \hat{r}(t)$ whose time derivative for $t \in [0,+\infty)$ is given as

$$\begin{aligned}
\dot{W}_i = & \frac{(\hat{\mathbf{c}}-\mathbf{p}_i)^\top(\dot{\hat{\mathbf{c}}}-\dot{\mathbf{p}}_i)}{\hat{D}_i^c} - \dot{\hat{r}} \\
= & -\frac{(\hat{\mathbf{c}}-\mathbf{p}_i)^\top}{\hat{D}_i^c}\delta((\hat{D}_i^c - \hat{r} - \frac{1}{\delta}\dot{\hat{r}})\boldsymbol{\psi}_i + \beta_i\hat{D}_i^c E\boldsymbol{\psi}_i) - \dot{\hat{r}} \\
= & -\frac{(\hat{\mathbf{c}}-\mathbf{p}_i)^\top}{\hat{D}_i^c}\boldsymbol{\psi}_i\delta(\hat{D}_i^c - \hat{r} - \frac{1}{\delta}\dot{\hat{r}}) - \frac{(\mathbf{c}-\mathbf{p}_i)^\top}{\hat{D}_i^c}E\boldsymbol{\psi}_i\delta\beta_i\hat{D}_i^c - \dot{\hat{r}} \\
= & -\delta(\hat{D}_i^c - \hat{r} - \frac{1}{\delta}\dot{\hat{r}}) - \dot{\hat{r}} = -\delta W_i.
\end{aligned}$$

   Hence for $t \in [0,+\infty)$, we have $\hat{D}_i^c(t) = \delta W_i(0)e^{-t} + \hat{r}(t)$ which implies W_i is converging to zero exponentially.
3. Finally, we show that the angle between the USVs will converge to the average consensus for n USVs, $\beta_i = \frac{2\pi}{n}$, so (23) holds. Firstly, note that we can write an angle between two vectors $\beta_i = \angle(v_2, v_1)$ as

$$\beta_i = 2\,\mathrm{atan2}((v_1 \times v_2)\cdot z, \|v_1\|\|v_2\| + v_1 \cdot v_2) \tag{24}$$

   and its derivative as

$$\dot{\beta}_i = \frac{\hat{v_1}\times z}{\|v_1\|}\dot{v_1} - \frac{\hat{v_2}\times z}{\|v_2\|}\dot{v_2} \tag{25}$$

   where $z = \frac{v_1\times v_2}{\|v_1\times v_2\|}, \hat{v_i} = \frac{v_i}{\|v_i\|}, i = 1,2$.
   Then, for $v_1 = \mathbf{p}_i - \hat{\mathbf{c}}$ and $v_2 = \mathbf{p}_{i+1} - \hat{\mathbf{c}}$ we get

$$\begin{aligned}
\dot{\beta}_i = & \frac{\hat{v_1}\times z}{\|v_1\|}\dot{v_1} - \frac{\hat{v_2}\times z}{\|v_2\|}\dot{v_2} \\
= & \frac{\hat{v_1}\times z}{\|v_1\|}\delta((\hat{D}_i^c - \hat{r} - \dot{\hat{r}})\boldsymbol{\psi}_i + \beta_i\hat{D}_i^c E\boldsymbol{\psi}_i) \\
& - \frac{\hat{v_2}\times z}{\|v_2\|}\delta((\hat{D}_{i+1}^c - \hat{r} - \dot{\hat{r}})\boldsymbol{\psi}_{i+1} + \beta_{i+1}\hat{D_{i+1}^c} E\boldsymbol{\psi}_{i+1}) \\
= & \delta(-\beta_i + \beta_{i+1}), \qquad i = 1,\ldots,n-1 \\
\dot{\beta}_n = & \delta(-\beta_n + \beta_1).
\end{aligned}$$

   which can be written in a compact form as

$$\dot{\beta} = -\delta B^\top \beta \tag{26}$$

   where B is the incidence matrix of the directed ring graph from v_1 to v_n. First, we note that the system (26) is positive (see e.g., [16]), i.e., $\beta_i(t) \geq 0$ if $\beta_i(0) \geq 0$ for all $t \geq 0$ and $i \in$. This proves the positions of the USVs are not interchangeable. Second, noticing that $B^\top$ is the (in-degree) Laplacian of the directed ring graph which is strongly connected, then by Theorem 6 in [17], β converges to consensus $\frac{2\pi}{n}\mathbb{1}$. ■

Remark 1. Note how the USV A_i will necessarily maintain its relative position $\mathbf{p}_i$ throughout the circumnavigation mission. In fact, we can prove that USV A_i is always in position $\mathbf{p}_i$.

Remark 2. Note that the p.e. condition is assumed for Theorem 1 and not proved. However, in the results section we will verify if the p.e. assumptions are true for our simulations, within the simulation time.

5 Numerical results

In this section, we present simulations for the protocol designed in Section 3. We use the derived method for estimation of the target (9) and (16) and the controlling protocol for the USVs (18). For this section, we discretize the whole algorithm to be able to use it computationally. The first subsection takes into account the persistent excitation condition and the second subsection analyses what happens when this condition is not verified.

5.1 Simulations with p.e. guarantees

In this subsection, we simulate a moving target with initial position $(x(0), y(0)) = (25, 25)$, radius $r(0) = 10$ and dynamic according to

$$\begin{aligned} x(t+1) &= x(t) + \alpha_1(t) + 0.5 \\ y(t+1) &= y(t) + \alpha_2(t) + 0.5 \\ r(t+1) &= r(t) + \alpha_3(t). \end{aligned} \tag{27}$$

However, we simulate that the UAV will provide as an initial noisy estimate of $(\hat{x}(0), \hat{y}(0)) = (25, 25)$, radius $\hat{r}(0) = 20$. Note that at time $t = 0$ the radius estimate is double the real radius.

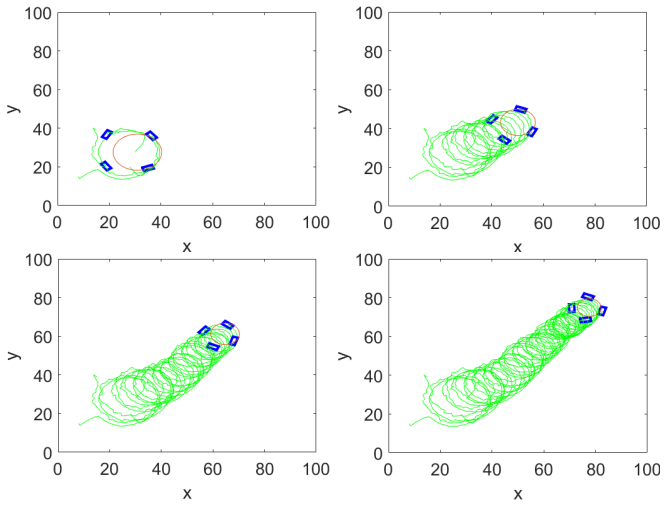

Fig. 4: Time-lapse of four USVs (blue rectangles) circumnavigating a moving target (red) with representation of their paths (green)

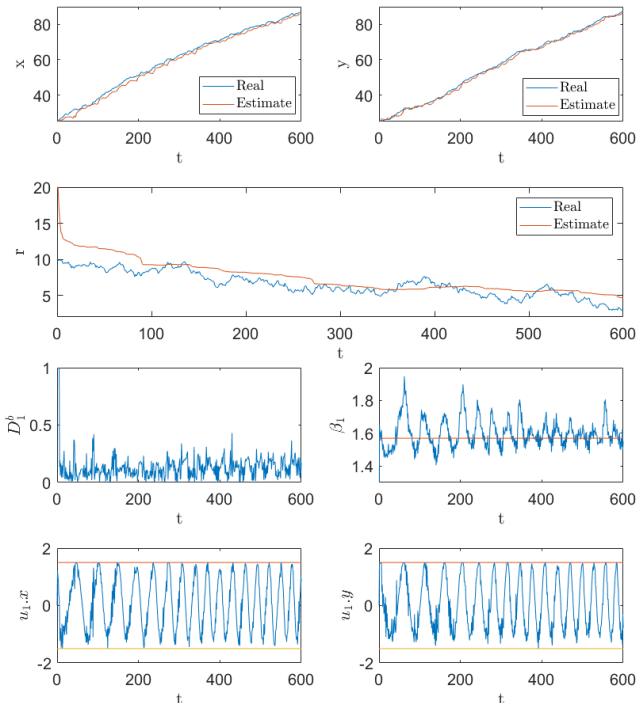

Fig. 5: First and second row: real and estimated target's centre $\mathbf{c} : x, y$ and radius r. Third row: tracking error of USV A1, D_1^b and angle β_1. Fourth row: control input of USV A1, $\mathbf{u}_1 : x, y$

Here, $\alpha_i(t)$ is a random scalar drawn from the uniform distribution within the interval of $[-0.5, 0.5]$ for $i = 1, 2, 3$. For this generated target we got the following results. In Fig. 4 the USVs circumnavigate the moving target. In Fig. 5 we have 7 plots. On the first and second row we compare the real and estimated target. Note that the estimate of the centre $\hat{\mathbf{c}}(\hat{x}, \hat{y})$ has an estimation error of up to 2 units. Also note that the estimate of the radius $\hat{r}$ is composed of two instances. In the first, the initial estimate provided by the UAV was very noisy and so we can see the estimate converging rapidly to a more accurate estimation. In the second we can see an estimation error of up to 2 units.

On the third row left column, we can see the distance D_i^b of each target to the boundary of the target - the perfect tracking would result in a distance D_i^b of 0 for all USVs, for every time step. Here we have an error of up to 0.5 units, except for the very beginning where the error can reach 10 units. This is merely because in the beginning the USVs are far away from the target. On the third row right column, we have the angle between USV A1 and A2, β_1. Having 4 USVs, the perfect tracking would result in $2\pi/4 = \pi/2 \approx 1.57$ for all USVs, for every time step. We can see this reference as the red line in the plot so we see that, for USV A1, the error is up to 0.2 radians.

Finally, on the fourth row we have the control input of USV A1, both in x and y in blue. Recall Remark. 2 where we stated that, for a practical implementation,

there should be a maximum velocity u_{max}. For this case study we defined that $u_{max} = 1.5$ and we plotted this limit in red. Note how the control input stays within the limit values 1.5 and -1.5.

Since we considered as an assumption that $\dot{\mathbf{p}}_1(t)$ and $\dot{D}_1^c(t)$ are p.e., we will evaluate whether they hold for this simulation example. According to [18], we can adapt Definition 2. to the discrete time case so we obtain the functions

$$f_{\dot{\mathbf{p}}_1}(t) = \sum_{k=t}^{t+m} \dot{\mathbf{p}}_1^\top(k)\dot{\mathbf{p}}_1(k), \quad f_{\dot{D}_1^c}(t) = \sum_{k=t}^{t+m} \dot{D}_1^c(k)^2, \tag{28}$$

which must fulfill $\rho_2 > f_{\dot{\mathbf{p}}_1}(t) > \rho_1$ and $\rho_4 > f_{\dot{D}_1^c}(t) > \rho_3$ for positive ρ_i.

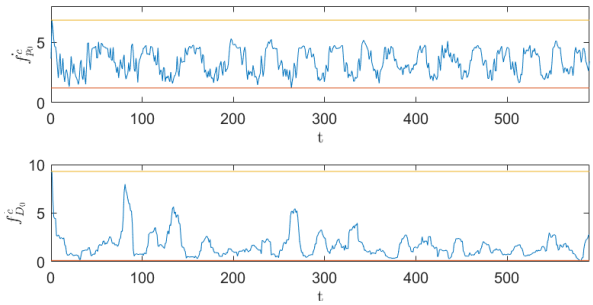

Fig. 6: First row: $f_{\dot{\mathbf{p}}_1}(t)$ is bounded by strictly positive bounds. Second row: $f_{\dot{D}_1^c}(t)$ is bounded by strictly positive bounds.

As seen in Fig. 6., these conditions are fulfilled for $\rho_1 = 1.1026$, $\rho_2 = 6.8371$, $\rho_3 = 0.2443$ and $\rho_4 = 8.8497$. Then, for these results in this simulating time span, the p.e. conditions hold.

5.2 Simulations without p.e. guarantees

In this subsection, we simulate a static target with position $(x(0), y(0)) = (25, 25)$ and radius $r(0) = 10$. As in the previous subsection, we simulate that the UAV provides an estimate of $(\hat{x}(0), \hat{y}(0)) = (25, 25)$ and radius $\hat{r}(0) = 20$.

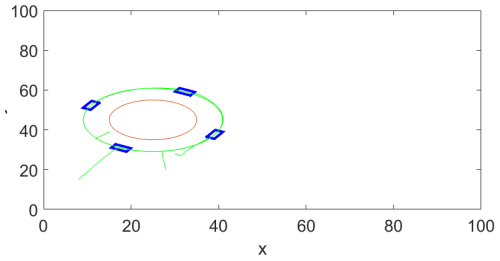

Fig. 7: Four USVs (blue rectangles) circumnavigating a moving target (red) with representation of their paths (green)

As seen in Fig. 7, the estimation of the position seems correct but the estimation of the radius seems wrong.

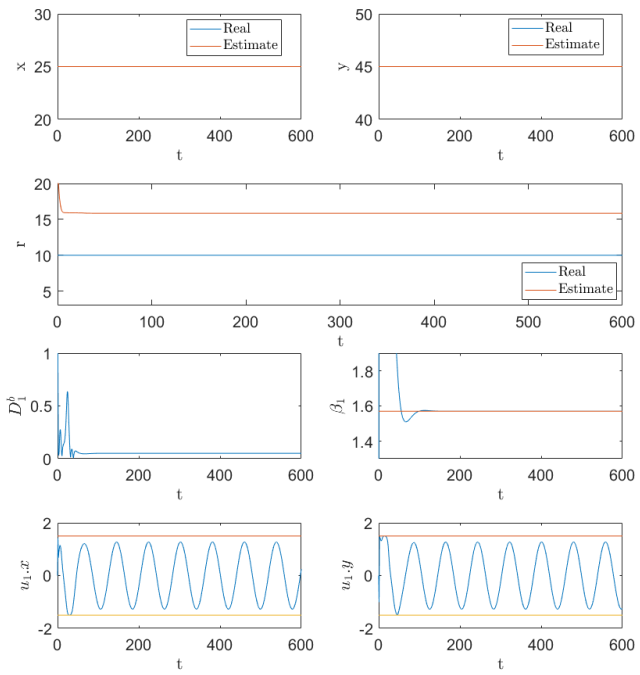

Fig. 8: First and second row: real and estimated target's centre $\mathbf{c} : x, y$ and radius r. Third row: tracking error of USV A1, D_1^b and angle β_1. Fourth row: control input of USV A1, $\mathbf{u}_1 : x, y$

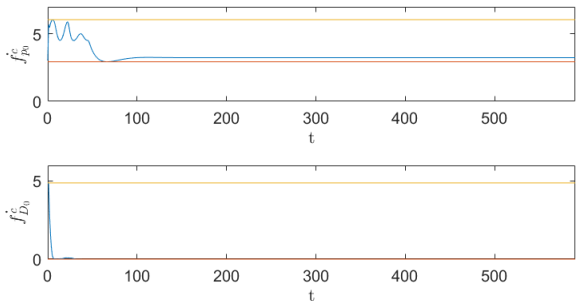

Fig. 9: First row: $f_{\dot{\mathbf{p}}_1}(t)$ is bounded by strictly positive bounds. Second row: $f_{\dot{D}_1^c}(t)$ is bounded by a strictly positive bound and zero.

From the first row Fig. 8 we can see how the estimates for the centre $\mathbf{c}(x, y)$ are correct for all the simulation time. However, from the second row we can see a steady state error for the estimation of r. Recall that the estimators derived in Section 3 for $\mathbf{c}$ and r rely on the p.e. conditions for $\dot{\mathbf{p}}_1$ and $\dot{D}_1^c$, respectively. Then, it seems that the p.e. condition on $\dot{D}_1^c$ does not hold, and, therefore, the estimation of r does not convergence to the real r. In fact, observing Fig. 9 we can conclude that, for this simulation time, even though the p.e. condition is verified for $\dot{\mathbf{p}}_1$, it is not verified for D_1^c since for some time t the minimum bound is not strictly positive.

6 Conclusions

We designed an algorithm that guarantees circumnavigation of an irregular shape approximated by a circle up to a bounded error. The algorithm relies on one UAV and a number of USVs according to the size of the target and to the importance of monitoring its fronts. Then, the proposed control protocol was proven to converge up to a bounded error assuming $\dot{\mathbf{p}}_1(t)$ and $\dot{D}_1^c(t)$ to be p.e.

As future work, we would like to exploit the circumnavigating USVs as in-site measuring vehicles. In order to do so, we are studying the hypothesis of using USVs capable of measuring the concentration of algal. This applies for the case in which we wish to monitor harmful algal blooms.

References

1. A. Sivertsen, S. Solbø, R. Storvold, A. Tøllefsen, and K.-S. Johansen, "Automatic mapping of sea ice using unmanned aircrafts," *ReCAMP Flagship Workshop*, p. 30, 2016.
2. A. Lucieer, D. Turner, D. H. King, and S. A. Robinson, "Using an unmanned aerial vehicle (uav) to capture micro-topography of antarctic moss beds," *International Journal of Applied Earth Observation and Geoinformation*, vol. 27, p. A:53 – 62, 2014.
3. A. Zolich, D. Palma, K. Kansanen, K. Fjørtoft, J. Sousa, K. H. Johansson, Y. Jiang, H. Dong, and T. A. Johansen, "Survey on communication and networks for autonomous marine systems," *Journal of Intelligent & Robotic Systems*, Apr 2018. [Online]. Available: https://doi.org/10.1007/s10846-018-0833-5
4. M. Egerstedt and X. Hu, "Formation constrained multi-agent control," *IEEE transactions on robotics and automation*, vol. 17, no. 6, pp. 947–951, 2001.
5. D. V. Dimarogonas and K. H. Johansson, "On the stability of distance-based formation control," in *2008 46th IEEE Conference on Decision and Control*. IEEE, 2008, pp. 1200–1205.
6. M. Cao, A. S. Morse, C. Yu, B. Anderson, and S. Dasgupta, "Controlling a triangular formation of mobile autonomous agents," in *2007 46th IEEE Conference on Decision and Control*. IEEE, 2007, pp. 3603–3608.
7. A. S. Matveev and K. S. Ovchinnikov, "Distributed communication-free control of multiple robots for circumnavigation of a speedy unpredictably maneuvering target," *2018 European Control Conference (ECC)*, pp. 1797–1802, 2018.
8. Z. Sun, *Cooperative Coordination and Formation Control for Multi-agent Systems*, ser. Springer Theses. Springer International Publishing, 2018.
9. A. Franchi, P. Stegagno, and G. Oriolo, "Decentralized multi-robot encirclement of a 3d target with guaranteed collision avoidance," *Autonomous Robots*, vol. 40, 07 2015.
10. M.-Y. Ani Hsieh, V. Kumar, and L. Chaimowicz, "Decentralized controllers for shape generation with robotic swarms," *Departmental Papers (MEAM)*, vol. 26, 09 2008.
11. G. Li, D. St-Onge, C. Pinciroli, A. Gasparri, E. Garone, and G. Beltrame, "Decentralized progressive shape formation with robot swarms," *Autonomous Robots*, pp. 1–17, 10 2018.

12. I. Shames, S. Dasgupta, B. Fidan, and B. D. O. Anderson, "Circumnavigation using distance measurements under slow drift," *IEEE Transactions on Automatic Control*, vol. 57, no. 4, pp. 889–903, 2012.
13. J. Fonseca, J. Wei, K. H. Johansson, and T. A. Johansen, "Cooperative decentralized circumnavigation with application to algal bloom tracking," in *IEEE/RSJ International Conference on Intelligent Robots and Systems, 2019.*
14. B. Anderson, "Exponential stability of linear equations arising in adaptive identification," *IEEE Transactions on Automatic Control*, vol. 22, no. 1, pp. 83–88, 1977.
15. N. Shimkin and A. Feuer, "Persistency of excitation in continuous-time systems," *Systems & Control Letters*, vol. 9, no. 3, pp. 225 – 233, 1987.
16. L. Farina and S. Rinaldi, *Positive Linear Systems: Theory and Applications*, ser. A Wiley-Interscience publication. Wiley, 2000.
17. J. Wei, X. Yi, H. Sandberg, and K. H. Johansson, "Nonlinear consensus protocols with applications to quantized communication and actuation," *IEEE Transactions on Control of Network Systems*, 2018.
18. K. J. Åström, *Adaptive Control.* Berlin, Heidelberg: Springer Berlin Heidelberg, 1991, pp. 437–450. [Online]. Available: https://doi.org/10.1007/978-3-662-08546-2_24